

05

## Spectral measurements of a niobium Josephson junction array by a superconducting receiver with a mixer based on high-temperature bicrystalline junction

© M.A. Galin,<sup>1</sup> L.S. Revin,<sup>1,2</sup> A.V. Samartsev,<sup>1,2</sup> M.Yu. Levichev,<sup>1</sup> A.I. El'kina,<sup>1</sup> D.V. Masterov,<sup>1</sup> A.E. Parafin<sup>1</sup>

<sup>1</sup>Institute for Physics of Microstructures, Russian Academy of Sciences, 603087 Nizhny Novgorod, Russia

<sup>2</sup>Alekseev State Technical University, 603087 Nizhny Novgorod, Russia  
e-mail: galin@ipmras.ru

Received May 13, 2024

Revised May 13, 2024

Accepted May 13, 2024

Spectral measurements of a niobium Josephson junctions array were performed to estimate the Josephson radiation linewidth. The array consists of 9996 Nb/NbSi/Nb junctions connected in series, occupying an area of  $5 \times 7 \text{ mm}^2$  on a silicon substrate. To analyze the Josephson spectrum, a heterodyne superconducting receiver with a mixer based on a high-temperature superconducting Josephson junction was used. Significant decrease of the linewidth to 0.3–0.8 MHz was detected, when the array is connected to an autonomous power source.

**Keywords:** Josephson junctions, HTSC, heterodyne receiver, spectrum, synchronization, terahertz emission

DOI: 10.61011/TP.2024.07.58800.166-24

### Introduction

Josephson junctions may be suitable for solution of many important fundamental and practical problems in physics: from supersensitive detection of a magnetic field [1a] and frequency standardization [1b] to quantum calculations [1c] and investigation of the Majorana bound states [1d]. Unusual effects occurring in the Josephson junctions result from coherent movement of the Cooper pairs through a barrier between the superconducting electrodes. One of the most beneficial effects is the AC Josephson effect that correlates the constant voltage on electrodes  $V$  with the fundamental frequency of the Josephson generation  $f_J$  only through fundamental constants. Typical values of  $V$  are corresponded by  $f_J$  covering the range from hundreds of GHz to tens of THz. For such range, there is still a problem of creation of compact and tunable radiation generators that was named as the terahertz gap problem [2]. Single Josephson junction emits a power hardly exceeding 1 pW (only if the junction is not distributed) [3], therefore the junctions shall be grouped in arrays and phase locked to achieve the power required for practical applications. The junction arrays satisfy the compactness and tunability criteria in a certain way and, therefore, may be treated as one of the terahertz gap problem solutions.

The issue of synchronization of junctions in arrays may be solved by investigating the spectrum of Josephson oscillation because the width of spectral line  $\Delta f$  is directly related to the number  $N_s$  of synchronized junctions usually as  $\Delta f \sim 1/N_s$  or  $\Delta f \sim 1/N_s^2$  [4]. The results of spectral measurements will make it possible to choose the best topology of the array facilitating the most effective synchro-

nization of junctions that leads to the increase of the output power. The Fourier spectroscopy method is widely used for examination of internal Josephson junctions in mesas of  $\text{Bi}_2\text{Sr}_2\text{CaCu}_2\text{O}_{8+\delta}$  (BSCCO) crystals [5–9]. However, the resolution of the standard Fourier spectrometers is from 1 to 10 GHz, which is usually insufficient for linewidth measurement, and they are mainly used to investigate the types of resonant modes excited in the BSCCO mesas.

Higher frequency resolution is provided by heterodyne-type receivers. Among them, a receiver with mixer based on a superconductor-insulator-superconductor (SIS) junction shall be distinguished. This receiver has a record-breaking sensitivity at the quantum noise level and high resolution together with tunability in a wide frequency range [10]. A SIS-based receiver was used to measure an oscillation linewidth of BSCCO mesas [11], long (distributed) Josephson junction [12,13], and discrete niobium junction array [14,15]. In [15] measurements on a superwavelength array containing 9996 niobium junctions were performed in a wide frequency range of  $\sim 200$ –300 GHz. It was found that the Josephson oscillation linewidth is affected significantly by technical noises from measurement devices. Typical values of  $\Delta f$  for the fundamental harmonic were from 3 to 6 MHz, however, after implementation of measures to eliminate technical noises the spectral linewidth was successfully reduced to 1.5 MHz.

In this work the Josephson radiation linewidth is investigated with the use of a heterodyne receiver where the mixer is a bicrystal Josephson junction based on YBaCuO high-temperature superconductor (HTSC). Such receiver is a good alternative to a receiver with SIS mixer because

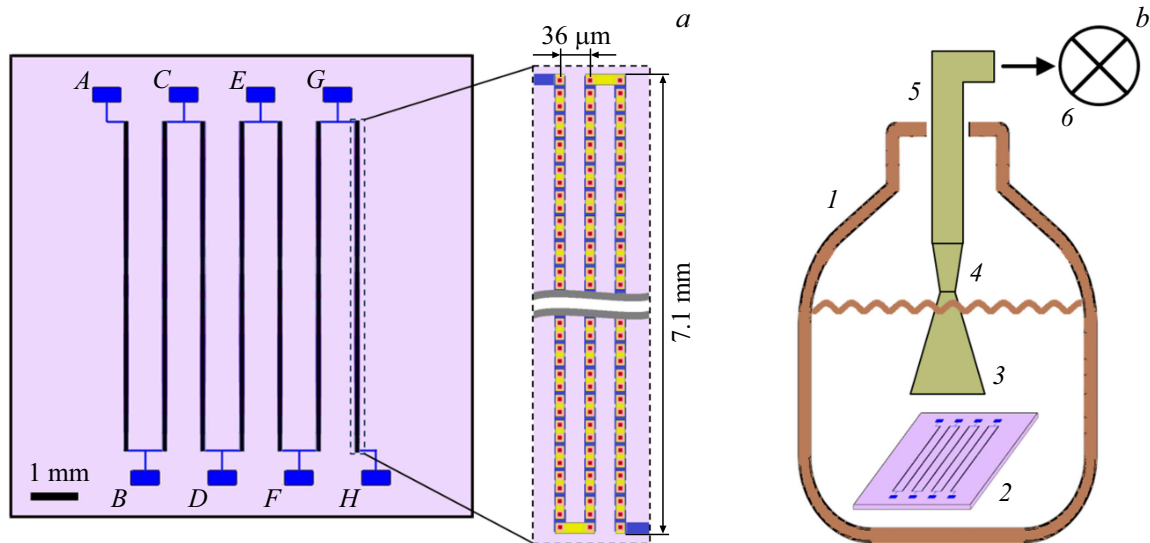


**Figure 1.** *a* — Topology of Josephson junction array. Letters from *A* to *H* denote contact pads enabling to connect individual sections of the array to power supply. The inset shows one of the sections with indication of the section length and distance between the single-strip lines. Each line contains 476 Nb/NbSi/Nb junctions (squares in the single-strip lines). *b* — Scheme of output of the Josephson radiation: *1* — liquid helium dewar, *2* — chip with junction array, *3* — square horn, *4* — waveguide taper to  $3.1 \times 1.55$  mm (required for suppression of higher modes in the waveguide), *5* —  $11 \times 5.5$  mm oversized waveguide, *6* — HTSC mixer.

it has important advantages [16]. It operates at higher temperatures up to the liquid nitrogen boiling point, which might reduce its cooldown cost significantly. It also features high nonlinearity making it possible to mix the signal with heterodyne's high harmonics. This capability may be very useful in view of the above-mentioned difficulties with the creation of tunable generators in a submillimeter band [2]. A discrete niobium junction array studied in [15] was chosen as an object of investigation. Spectral measurements were performed within the range of 160–240 GHz, including at different number of active junctions in the array. When an autonomous power source is connected to the array instead of the current source, considerable reduction of the Josephson oscillation linewidth to 0.3–0.8 MHz is observed.

## 1. Topology of the array and output of the Josephson radiation

The investigated series array of 9996 Josephson junctions is placed on a  $1 \times 1$  cm silicon substrate of 0.38 mm in thickness (Figure 1, *a*). The array is divided into 7 sections spaced at 0.75 mm. Each section consists of 3 single-strip lines of 7.1 mm in length, each of them contains 476 junctions. Center-to-center distance between the adjacent lines is  $36 \mu\text{m}$ . Dimensions of junction are  $8 \times 8 \mu\text{m}$ . Material of junction is niobium and silicon compound with atomic content of niobium of about 10%. On the ends of the array and between sections, there are contact pads designed to connect to the power supply circuit the whole array or several adjacent sections. The array is fabricated using the electron-beam lithography and reactive ion etching methods [17,18].

This chip was immersed in the liquid helium dewar. The Josephson radiation was output from the neck of the dewar via the waveguide path placed inside a metal tube of about 1 m in length (Figure 1, *b*). The chip was placed at the bottom end of the path opposite to the  $13 \times 13$  mm aperture of the square horn. The chip was protected against spurious magnetic fields by a cylindrical permalloy screen. The main part of the path was a  $11 \times 5.5$  mm rectangular waveguide. It is oversized in the investigated frequency range allowing the radiation absorption on the waveguide walls to be reduced. For more detailed description of the scheme of output of the Josephson radiation, see [15].

## 2. Measurement scheme

The HTSC Josephson mixer was a YBaCuO superconductor film sputtered on a surface of the  $\text{Zr}_{1-x}\text{Y}_x\text{O}_2$  bicrystal substrate with a disorientation angle of a single-crystal lattice of  $24^\circ$  in [001] plane. The Josephson junction was formed at the single-crystal boundary, its thickness was  $0.1 \mu\text{m}$ , and width was  $1.5 \mu\text{m}$ . The junction is integrated into a log-periodic planar antenna [19] for broadband coupling with the external radiation (the inset in Figure 2, *a*).

Spectral measurements were carried out using two basic schemes (Figure 2). In both cases, the HTSC mixer was attached to a silicon hyper-hemispherical lens and was installed into the Gifford-McMahon closed-cycle cryostat. The mixer was cooled to a temperature of 6–7 K. In the first scheme R&S SMB100A low-frequency (LF) generator was used as a heterodyne signal source (Figure 2, *a*). The

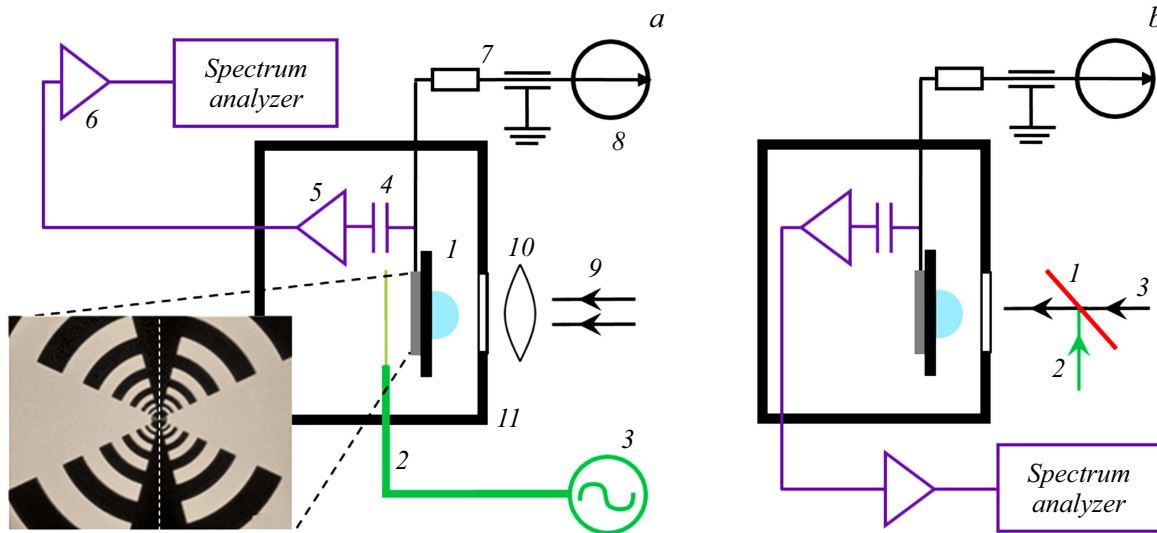


**Figure 2.** Two spectral measurement schemes. *a* — Mixing scheme at high harmonic of LF heterodyne: 1 — HTSC mixer on a silicon lens, 2 — whip antenna, 3 — LF generator, 4 — isolating capacitor, 5 — cooled amplifier, 6 — room amplifier, 7 — low frequency filter, 8 — DC power supply, 9 — radiation of Josephson junction array, 10 — PTFE lens, 11 — cryostat. The inset — photo of the sample with YBaCuO mixer, where the dashed line shows the bicrystal boundary. *b* — Mixing scheme at the first/second harmonic of HF heterodyne: 1 — beam splitter, 2 — reference signal of BWO, 3 — radiation of Josephson junction array.

heterodyne signal arrived to a symmetric antenna placed near the mixer on the flat side of the silicon lens. The signal from the junction array was supplied from outside via a quasi-optical circuit with the external PTFE lens and IR filters installed on the optical window of the cryostat and was focused on the junction of the HTSC mixer junction by the silicon lens. The intermediate frequency (IF) signal was formed by means of mixing the Josephson radiation with high harmonics of the heterodyne signal (from 8th to 13th depending on the generation frequency of the array) and was then output via a coaxial cable to a spectrum analyzer. The IF signal was amplified by 52 dB using a pre-amplifier placed on a cold plate of the cryostat, and the room amplifier. The output noise was  $-64$  dBm in the frequency range of 1–3 GHz in the 3 MHz band of the spectrum analyzer. A battery-powered source was used for DC offset of the mixer.

The second measurement scheme employed a backward-wave oscillator (BWO) with a radiation range of 115–175 GHz as a reference signal source (Figure 2, *b*). In this case, signal mixing took place on the first or second harmonic of the heterodyne. The optional power of BWO was selected by a mechanical attenuator. A beam splitter made of mylar or PTFE thin film was used to mix the signals from the heterodyne and the array. This measurement scheme provided higher receiver sensitivity due to mixing on the first or second harmonic, but required finer and longer tuning compared with the scheme using the LF generator.

Preliminary characterization of the HTSC mixer, including the loss in the waveguide path, made it possible to estimate the conversion efficiency. Efficiency of mixing of 165 GHz signal on the first harmonic is  $-10$  dB, on the tenth harmonic is  $-29$  dB.

### 3. Results

Figure 3 shows the current-voltage curve (IVC) of the whole Josephson junction array (power supply is connected to contact pads A and H, see Figure 1), and IVC of the

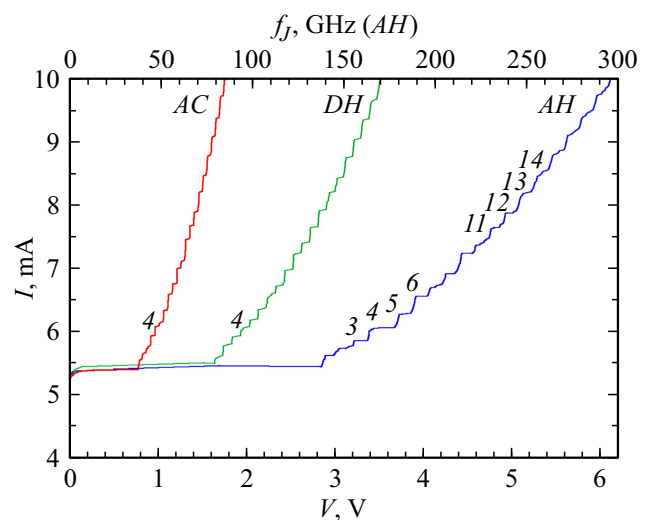


**Figure 3.** IVC of two sections (AC — contact pads A and C are connected, see Figure 1), four sections (DH) and all seven sections (AH) of the Josephson junction array. IVC were obtained with increasing bias current (direct branches). The upper axis denotes the averaged Josephson frequency  $f_J$  of the whole array (AH). To obtain  $f_J$  of array sections AC and DH, multiply the values on the top axis by  $7/2$  and  $7/4$ , respectively. Spectral measurements were performed on the numbered steps, numeration starts from  $f_J = 139$  GHz that is the beginning of the resistive branch of IVC of the array AH.

parts of the array: two (AC) and four (DH) sections. As seen from figure 3, the critical current of the array is  $I_c \approx 5.4\text{--}5.5\text{ mA}$ , the characteristic Josephson frequency is  $f_c \approx 140\text{ GHz}$ . A small variation of  $I_c$  within 0.1 mA observed when connecting different sections of the array is attributed to the spread of the junction parameters and to an uncontrollable capture of magnetic vortices by a small number of junctions. Each IVC demonstrates current steps occurring due to excitation of resonant modes by the Josephson radiation along the single-strip lines of the array [15,20,21]. Due to interaction of the junctions and resonance system, radiation at the steps is significantly enhanced. IVC of the whole array (AH) contains up to 24 such self-induced steps that completely decay at  $V \approx 7\text{ V}$ , which corresponds to  $f_J = 350\text{ GHz}$  (see [15], Figure 2, a). Hereinafter, the value  $f_J$  applied to the array means the Josephson frequency averaged by all junctions of the array and calculated accordingly to the fundamental Josephson relation [3] as  $f_J = KV/N$ , where  $K \approx 483.6\text{ GHz/mV}$ ,  $N$  is the number of junctions in the array (in this case it may be the whole array AH as well as its part). Relation between this quantity and the Josephson frequencies of individual junctions will be addressed below.

Spectral measurements were performed using both types of heterodyne: LF generator and BWO. Spectral lines of the Josephson radiation were observed at current steps from 3 to 6 covering the frequency range of  $f_J = 150\text{--}180\text{ GHz}$ , and at the steps from 11 to 14 that are corresponded by the range of  $f_J = 225\text{--}250\text{ GHz}$  (Figure 3). In the latter case the 2nd harmonic of BWO used as a reference signal. The specified intervals will be hereinafter referred to as the fundamental and high-frequency (HF) ranges of measurements, correspondingly. The strongest signal was observed in the fundamental range at 4th current step.

In the first series of measurements, the array was connected to Keithley 6221 current source [22], so that the constant current mode was implemented in the circuit with the array, i.e. in the equivalent circuit Keithley was an ideal current source with infinite resistance. All spectral measurements with this [15] and similar [23,24] niobium Josephson junction arrays were performed in this mode. Here, as in [15], it was concluded about a significant influence of noise on the measured spectra because the lines were poorly approximated by the Lorentz curve and often had asymmetric shape, wherein the linewidth was defined not only by the position of the operation point on IVC, but also by the configuration of the connected measurement devices. The spectral linewidth decreased insignificantly when the voltmeter and temperature controller, that were auxiliary devices during spectrum scanning, were disconnected from the measurement circuit. Within the fundamental range, the linewidth varied within 3–15 MHz. Figure 4, a shows typical spectral lines of the Josephson radiation recorded at the steps from 4 to 6 with the use BWO and LF generator as a heterodyne. As in [15,24], position of the lines were close to  $f_J$ . The spectral frequency deviated from  $f_J$  by no more than 1.5 GHz exceeding  $f_J$  in most cases.

Mismatch of these frequencies is explained by the presence of the Josephson junctions oscillating in the asynchronous regime in the vicinity of the nodes of resonant mode [21]. Compared with the remaining junctions in the proximity of the antinodes of the mode, their Josephson frequencies may differ considerably from the resonant frequency to which the spectrum peak corresponds.

In measurements in the HF range the linewidth increased up to 27 MHz. Note that [15] reported much narrower lines for this array in the same range — their width was 3–6 MHz. This mismatch additionally illustrates the significant influence of technical noise on the spectrum of the junction array. This influence varies in different conditions of the measurements — in this case noises broadened the spectral lines much more than in [15].

The measurements showed that position of spectral lines on the frequency axis was unstable in time. The oscillation amplitude of the lines was equal to 1–10 MHz and usually doesn't exceed the width of lines themselves. These are quite low-frequency oscillations because the typical frequency of such oscillations turns to be lower than the scanning frequency of spectrum lines which is no more than 1 kHz.

Due to frequency instability of spectral lines, the following procedure of measurement of the linewidth was chosen. From 4 to 20 implementations of the spectrum were scanned depending on the oscillation amplitude of the line and relative noise level. A segment containing the spectral line we are interested in was outlined on each implementation. Then the implementations were approximated by the Gaussian function using the least-square method to define the central frequency of each line. The final result was obtained by averaging the lines preliminary shifted by the mean value of central frequency. This measurement procedure prevents distortion of the frequency-shifted line that occurs inevitably during single scanning, and broadening of the line during simple averaging of implementations without considering the shift of the central frequency. All results presented in this work have been obtained using the specified method. The size of the noise band on the presented spectra varied from 20 to 100 pW and was defined by the number of operations of averaging, video bandwidth and level of the technical noises in the measurement system that could vary considerably for different reasons.

In the second measurement series the array was connected to the autonomous power source independent of household electrical network, that can be represented as a voltage source and a resistor of  $R_i = 1\text{ k}\Omega$  resistance connected in series. The current in the array was controlled by the voltage in the power source within  $\pm 10\text{ V}$ . With such power supply configuration, considerable decrease of the Josephson generation linewidth to values from 0.3 to 0.8 MHz was observed. The measurement result thus didn't depend either on the type of heterodyne of the receiver or on the frequency range. The typical examples of the corresponding spectra are given in Figure 4, b showing the lines

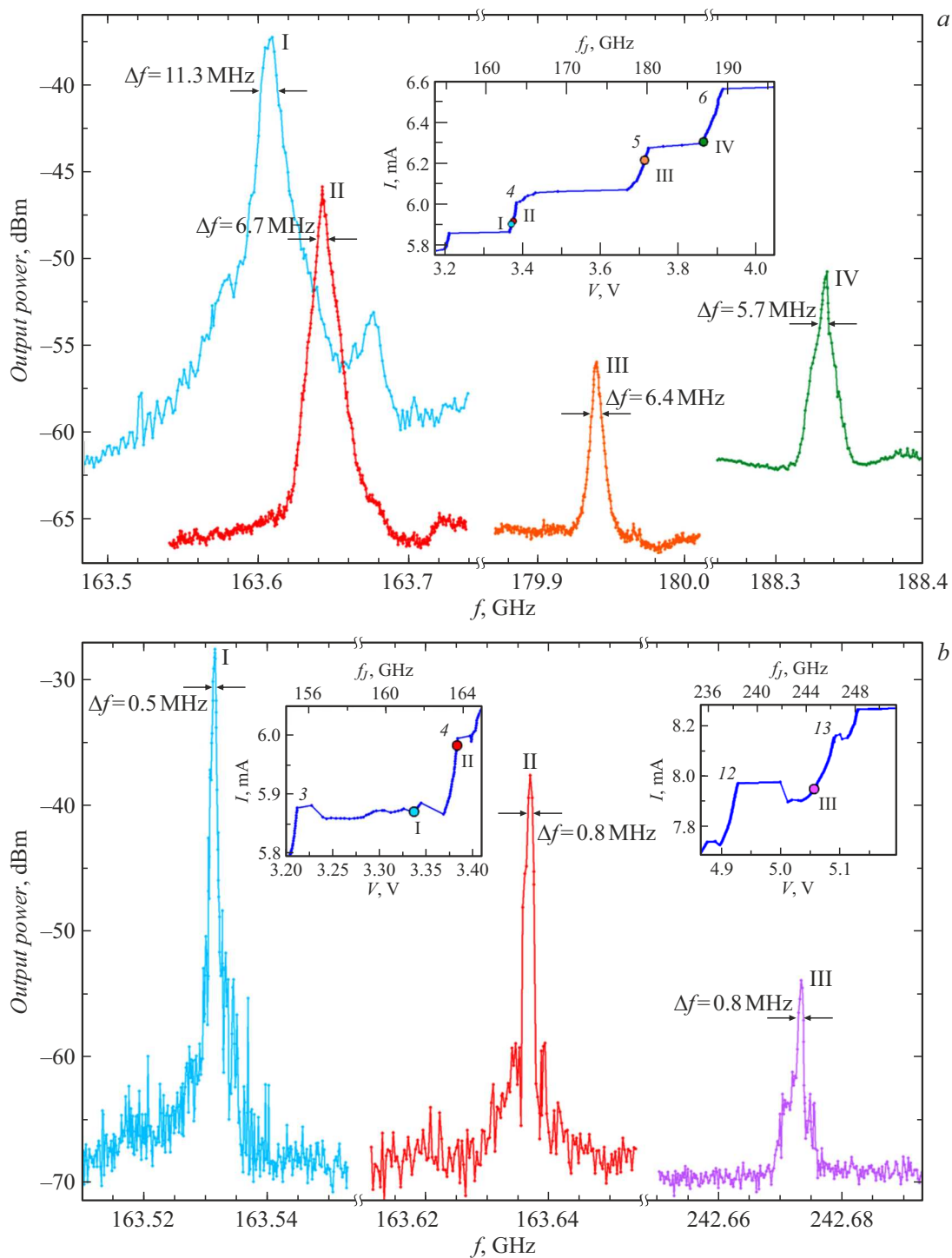


**Figure 4.** Spectral lines of the Josephson radiation when Keithley 6221 current source is connected to the array (a) and autonomous supply of the array (b). Lines I (a, b) were obtained with the use of fundamental harmonic of BWO as a heterodyne signal, line III (b) were obtained using the 2nd harmonic of BWO as such signal, and the other lines were obtained when the LF generator was used as a heterodyne. Linewidth measured at 1/2 from the maximum value is indicated at each line. Lines I and IV (a) were obtained at the resolution of spectral analyzer (RBW) of 3 MHz, lines II and III (a) — at the resolution of 1 MHz, all lines (b) — at the resolution of 300 kHz. The insets show the current steps of IVC with the operation points marked on them where the presented spectra were measured. The steps are numbered accordingly to Figure 3. Distortion of IVC (b) compared with IVC in Figure 3 is explained by the chosen scheme of supply of the array where the constant current mode is not implemented on some parts of IVC.

obtained within the fundamental range using both types of heterodyne, and also the line obtained in the HF range. Note that in this series of measurements the voltmeter and temperature controller were always disconnected from the measurement system.

The chosen autonomous supply circuit causes distortion of the IVC of the array compared with IVC obtained in the constant current mode (Figure 3). However, distortions occur only in the areas of IVC where differential resistance  $R_d$  significantly exceeds  $R_i$ . At the horizontal parts between steps  $R_d = 3\text{--}25\text{ k}\Omega$  that is much higher than  $R_i$ . As a result, local dips occur in these segments and also in transition from the superconducting branch to the resistive branch (see insets in Figure 4, *b*). The steps are distorted slightly because at them  $R_d = 100\text{--}500\ \Omega$ .

In one of the local dips before the 4th current step of IVC (Figure 4, *b*, left inset), a line at the fundamental harmonic of BWO was obtained. Nevertheless, frequency position of this line corresponds to the 4th step. Probably, a two-mode generation regime is implemented in this case, i.e. two resonant modes corresponding to the 3rd and 4th steps are excited in the array at once. The line corresponding to the 3rd mode was not scanned due to a limited frequency range of the spectrum analyzer. In the two-mode generation regime, the Josephson junctions are divided into two groups belonging to different modes. As a result, the Josephson frequency  $f_J$  averaged over the array turns to be between the current steps, that is observed on the corresponding parts of IVC. Other lines shown in Figure 4, *b*, like in the first series of measurements, deviate from  $f_J$  no more than 1.5 GHz.

Narrow lines were also observed when the autonomous power source was connected to the parts of the array containing from 2 to 5 sections. Measurements here were performed only at 4th current step of IVC where BWO was used as a heterodyne. Linewidths, similar to the case of the whole array, were equal to 0.3–0.8 MHz. Examples of lines obtained in the measurement on two (*AC*) and four (*DH*) sections are represented in Figure 5. Line *DH* near 163.7 and 163.73 GHz has local maxima that may be caused by the oscillations of the amplitude of the heterodyne signal.

Considerable narrowing of spectral lines in the second series of measurements is obviously attributed to the configuration of the power circuit of the array. Change to another type of power supply is the most obvious explanation: from the ideal current source to the voltage source with resistance connected in series. Spectrum variations in this array when the current source is changed to the voltage source have been already observed in the studies using a semiconductor heterodyne receiver [25]. Though these changes were of different nature probably due to a slower response of the measurement system, in [25] it was suggested that the spectral line considerably narrows at power supply from the voltage source. Autonomy of the power supply circuit, i.e. its independence from the household electrical network, may also be the reason of the narrowing of the line. Considerable variations of the spectral

linewidth in the first series of measurements described in this work and in the measurements described in [15] were explained exactly by the noise from the electrical network. Moreover, in the second series of measurements as mentioned above, the secondary devices were disconnected from the measurement circuit. Similar action resulted in some decrease of the linewidth of the spectral lines in the first series of measurements.

The width of the obtained spectral lines in the measurements with the autonomous power source was limited by the chosen resolution bandwidth (RBW) for the spectrum analyzer that was equal to 300 kHz. With further decrease of RBW, the line was smeared by noise due to the observed LF instability of the line on the frequency axis similar to the first series of measurements. The oscillation amplitude was also within 1–10 MHz. Thus, the spectral measurements essentially achieved the resolution limit, therefore the spectral lines of the Josephson radiation may be more narrow than the lines observed herein. Assuming that about 1000 junctions are synchronized in each section of the array (i.e. 70% of the total number of junctions in the section, which agrees with the numerical calculations in [21]), then, as follows from [4], the width of the line of generation from one section of the array shall not be more than 10 kHz (without considering that the sections can be also synchronized between each other). Limitation on the resolution of the spectral lines also prevented the adequate approximation of the lines by the Gaussian or Lorentz curves to estimate the influence of technical noises.

We can see several possible explanations of the observed LF instability of spectral lines. The same technical noises that causes broadening of the lines seems to be one of the obvious reasons, but now this might be noise converted to frequencies  $\leq 1\text{ kHz}$  due to nonlinear properties of the Josephson junctions, or flicker noise. However, amplitude of deviation 1–10 MHz typical for LF instability is corresponded by oscillations of induced current 1–10  $\mu\text{A}$ , that seems to be too high for noise. Another possible reason is the instability of synchronization of the Josephson junctions in the array. As shown in [21], the array may contain a certain fraction of asynchronous junctions placed in the vicinity of the nodes of the resonant mode. The number of synchronous and asynchronous junctions probably varies continuously that leads to the instability of the properties of the resonator and, as a consequence, to the offset of the resonant frequency. The reason of the LF instability may be also possible temperature oscillations in the array caused, for example, by turbulent convection flows in liquid helium [26].

Spurious electromagnetic impact on the array from components of the receiver is excluded as a cause of the LF instability. Radiation power of the BWO was from 20 to 40 mW, and this radiation is difficult to be completely isolated from the array (Figure 2, *b*). Considering the typical radiation power at the output of the array of about several  $\mu\text{W}$  [20], even a small fraction of radiation of the BWO entering the waveguide path for the Josephson



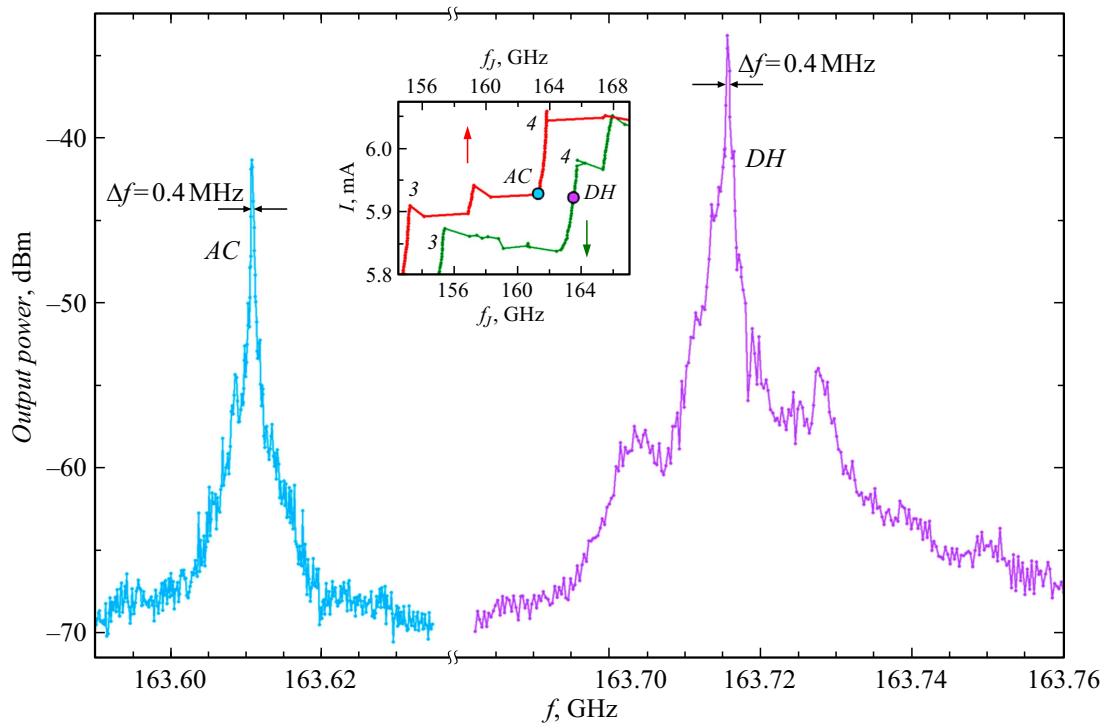


**Figure 5.** Spectral lines of the Josephson radiation obtained with the autonomous power source connected to two (*AC*) and four (*DH*) sections of the array. BWO was used as heterodyne for the measurements. The lines were obtained with the resolution bandwidth (RBW) of the spectrum analyzer of 300 kHz. The inset shows operation points in IVC where the spectra were observed. For each IVC, an averaged Josephson frequency is plotted on the horizontal axis instead of the voltage.

radiation may be expected to have a significant effect on the resonant mode and, thus, to shift the generation frequency of the array. However, the LF instability also takes place when using the LF generator (Figure 2, *a*), but its possible connection with the array is very indirect. The Josephson radiation was mixed with the 10th or a higher harmonic of signal of the LF generator. Investigations of a similar bicrystal junction show that the junction absorbs maximum  $4 \mu\text{W}$  with a comparable power of reference signal [27], and the power at the 10th harmonic reradiated by the junction, according to our calculations, will be lower by about 5 orders of magnitude and will be no more than 0.1 nW. Taking into account the measurement system configuration, radiation with a power lower by another 2 orders of magnitude will reach the array and only a small portion of this power will be absorbed by the array. It is obvious that the final power will be insufficient to produce a significant impact on the frequency of spectral line.

## Conclusion

The study has performed spectral measurements of the niobium Josephson junction array using the heterodyne superconductor receiver. The HTSC Josephson junction based on YBaCuO formed at the bicrystal interface of  $\text{Zr}_{1-x}\text{Y}_x\text{O}_2$  substrate served as a mixer in the receiver. When the array was supplied from the current source, spectral lines of the Josephson radiation were observed

and had a width from 3 to 15 MHz in the range of 150–180 GHz that increased up to 27 MHz in the range of 225–250 GHz. When the array was connected to the circuit with an autonomous voltage source and 1 k $\Omega$  series resistor, the linewidth decreased to 0.3–0.8 MHz at all measured frequencies and also when 2 to 5 sections of the array were connected. Significant narrowing of the spectral lines may be explained by the change in configuration of power supply of the array as well as by reduction of external noises at the reconnection of the source from household electrical network to the autonomous power source.

LF oscillations of spectral lines on the frequency axis are observed in all measurements. The amplitude of oscillations was 1–10 MHz, while the frequency didn't exceed 1 kHz. The LF oscillations didn't allow to obtain the lines with RBW lower than 300 kHz during the measurements with the autonomous power source. Therefore, the spectral linewidth may be smaller than the values observed in the present work. To improve the spectral resolution, it is necessary to increase the scan rate of spectrum.

The LF instability effect of the spectral lines of Josephson radiation requires additional study. This effect is an obstacle for potential application of the niobium Josephson junction arrays as a heterodyne. The problem of the frequency stabilization of the line may be solved by the development of a phase-locked-loop control system for these arrays similar to how this was done for the heterodyne of the superconductor integral receiver with SIS mixer [10].

## Acknowledgments

The authors are grateful to V.V. Kurin and V.A. Anfertiev for the useful discussions of the measurements, and also to O. Kieler for the sample fabrication.

## Funding

The study was supported by Center of Excellence „Center of Photonics“ funded by the Ministry of Science and Higher Education of the Russian Federation, contract № 075-15-2022-316 (development of the output scheme of the Josephson radiation, measurement of IVC the Josephson junction array) and by the Russian Science Foundation, project № 20-79-10384-P (spectral measurements with the use of the HTSC mixer).

## Conflict of interest

The authors declare that they have no conflict of interest.

## References

- [1] *Fundamentals and Frontiers of the Josephson Effect*, ed. by F. Tafuri (Springer Nature, Switzerland, AG, 2019); a — J. Gallop, L. Hao. Ch. **14**: *Physics and Applications of NanoSQUIDs*, p. 555–585; b — S.P. Benz. Ch. **15**: *Josephson Junctions for Metrology Applications*, p. 587–609; c — A.F. Kockum, F. Nori. Ch. **17**: *Quantum Bit with Josephson Junctions*, p. 703–741; d — D. Golubev, T. Bauch, F. Lombardi. Ch. **13**: *Josephson Effect in Graphene and 3D Topological Insulators*, p. 529–553.
- [2] M. Tonouchi. *Nature Photon.*, **1**, 97 (2007). DOI: 10.1038/nphoton.2007.3
- [3] M. Darula, T. Doderer, S. Beuven. *Supercond. Sci. Technol.*, **12** (1), R1 (1999). DOI: 10.1088/0953-2048/12/1/001
- [4] A.K. Jain, K.K. Likharev, J.E. Lukens, J.E. Sauvageau. *Phys. Rep.*, **109** (6), 309 (1984). DOI: 10.1016/0370-1573(84)90002-4
- [5] M. Ji, J. Yuan, B. Gross, F. Rudau, D.Y. An, M.Y. Li, X.J. Zhou, Y. Huang, H.C. Sun, Q. Zhu, J. Li, N.V. Kinev, T. Hatano, V.P. Koshelets, D. Koelle, R. Kleiner, W.W. Xu, B.B. Jin, H.B. Wang, P.H. Wu. *Appl. Phys. Lett.*, **105** (12), 122602 (2014). DOI: 10.1063/1.4896684
- [6] T.M. Benseman, A.E. Koshelev, V. Vlasko-Vlasov, Y. Hao, U. Welp, W.-K. Kwok, B. Gross, M. Lange, D. Koelle, R. Kleiner, H. Minami, M. Tsujimoto, K. Kadowaki. *Phys. Rev. B*, **100** (14), 144503 (2019). DOI: 10.1103/PhysRevB.100.144503
- [7] T. Kashiwagi, T. Yuasa, G. Kuwano, T. Yamamoto, M. Tsujimoto, H. Minami, K. Kadowaki. *Materials*, **14** (5), 1135 (2021). DOI: 10.3390/ma14051135
- [8] R. Kobayashi, K. Hayama, S. Fujita, M. Tsujimoto, I. Kakeya. *Phys. Rev. Appl.*, **17** (5), 054043 (2022). DOI: 10.1103/PhysRevApplied.17.054043
- [9] H. Sun, S. Chen, Y.-L. Wang, G. Sun, J. Chen, T. Hatano, V.P. Koshelets, D. Koelle, R. Kleiner, H. Wang, P. Wu. *Appl. Sci.*, **13** (6), 3469 (2023). DOI: 10.3390/app13063469
- [10] V.P. Koshelets, S.V. Shitov. *Supercond. Sci. Technol.*, **13** (5), R53 (2000). DOI: 10.1088/0953-2048/13/5/201
- [11] M. Li, J. Yuan, N.V. Kinev, J. Li, B. Gross, S. Guénon, A. Ishii, K. Hirata, T. Hatano, D. Koelle, R. Kleiner, V.P. Koshelets, H. Wang, P. Wu. *Phys. Rev. B*, **86** (6), 060505 (2012). DOI: 10.1103/PhysRevB.86.060505
- [12] N.V. Kinev, K.I. Rudakov, L.V. Filippenko, A.M. Baryshev, V.P. Koshelets. *IEEE Trans. Terahertz Sci. Technol.*, **9** (6), 557 (2019). DOI: 10.1134/S1063783420090140
- [13] N.V. Kinev, K.I. Rudakov, L.V. Filippenko, V.P. Koshelets. *IEEE Trans. Appl. Supercond.*, **32** (4), 1500206 (2022). DOI: 10.1109/TASC.2022.3143483
- [14] F. Boussaha, M. Salez, A. Féret, B. Lecomte, C. Chaumont, M. Chaubet, F. Dauplay, Y. Delorme, J.-M. Krieg. *J. Appl. Phys.*, **105** (7), 073902 (2009). DOI: 10.1063/1.3099602
- [15] M.A. Galin, N.V. Kinev, M.Yu. Levichev, A.I. El'kina, A.V. Antonov, A.V. Khudchenko, G.P. Nazarov, V.V. Kurin, V.P. Koshelets. *IEEE Trans. Appl. Supercond.*, **34** (3), 1100405 (2024). DOI: 10.1109/TASC.2024.3386416
- [16] M. Malnou, C. Feuillet-Palma, C. Ulysse, G. Faini, P. Febvre, M. Sirena, L. Olanier, J. Lesueur, N. Bergeal. *J. Appl. Phys.*, **116** (7), 074505 (2014). DOI: 10.1063/1.4892940
- [17] F. Mueller, R. Behr, T. Weimann, L. Palafox, D. Olaya, P.D. Dresselhaus, S.P. Benz. *IEEE Trans. Appl. Supercond.*, **19** (3), 981 (2009). DOI: 10.1109/TASC.2009.2019063
- [18] O. Kieler, R. Wendisch, R.-W. Gerdau, T. Weimann, J. Kohlmann, R. Behr. *IEEE Trans. Appl. Supercond.*, **31** (5), 1100705 (2021). DOI: 10.1109/TASC.2021.3060678
- [19] E.I. Glushkov, A.V. Chiginev, L.S. Kuzmin, L.S. Revin. *Beilstein J. Nanotechnol.*, **13**, 325 (2022). DOI: 10.3762/bjnano.13.27
- [20] M.A. Galin, A.M. Klushin, V.V. Kurin, S.V. Seliverstov, M.I. Finkel, G.N. Goltsman, F. Mueller, T. Scheller, A.D. Semenov. *Supercond. Sci. Technol.*, **28** (5), 055002 (2015). DOI: 10.1088/0953-2048/28/5/055002
- [21] M.A. Galin, I.A. Shereshevsky, N.K. Vdovicheva, V.V. Kurin. *Supercond. Sci. Technol.*, **34** (7), 075005 (2021). DOI: 10.1088/1361-6668/abfd0b
- [22] Electronic media. Available at: <https://download.tek.com/datasheet/6220-6221.pdf>
- [23] F. Song, F. Müller, R. Behr, A.M. Klushin. *Appl. Phys. Lett.*, **95** (17), 172501 (2009). DOI: 10.1063/1.3253417
- [24] M.A. Galin, V.V. Kurin, I.A. Shereshevsky, N.K. Vdovicheva, A.V. Antonov, B.A. Andreev, A.M. Klushin. *IEEE Trans. Appl. Supercond.*, **31** (5), 1500905 (2021). DOI: 10.1109/TASC.2021.3064533
- [25] M.A. Galin, M.Yu. Levichev, A.I. El'kina, A.V. Antonov, O. Kieler. *Proceedings of XXVII International Symposium „Nanophysics and Nanoelectronics“* (Nizhny Novgorod, Russia, 2023), vol. 1, p. 25.
- [26] A. Libchaber. *Physica B+C*, **109–110**, 1583 (1982). DOI: 10.1016/0378-4363(82)90181-4
- [27] E. Matrozova, A. Parafin, D. Masterov, L. Revin, S. Pavlov. *Proceedings of 2022 IEEE 8th All-Russian Microwave Conference (RMC)* (Russia, Moscow, November 23–25, 2022), p. 45. DOI: 10.1109/RMC55984.2022.10079648

Translated by E. Ilinskaya